Measurement of Bubble Size, Gas holdup and Interfacial Area in Bubble Columns using Image Processing Techniques

Agarwal, N., Verma, A. K.

Abstract*: Bubble sizes in bubble column affect transfer processes. Therefore, it's important to calculate bubble size and interfacial area. Bubble size distribution (BSD) in a bubble column of rectangular cross section with dimensions 0.2m x 0.02m was measured using photographic method (400 fps) for air-water system. Gas holdup, Sauter-mean bubble diameter, aspect ratio and specific interfacial area were estimated from BSD. Effect of superficial gas velocity and static bed height on these parameters was investigated. The bubble size distribution exhibited mono-modal distribution showing the presence of non-uniform homogeneous bubbling regime. The frames of video were analysed using image processing steps to obtain major and minor axis of elliptical bubbles. Values of d_{32}, ε, and a_i were estimated from the data. The value of d_{32} increased with increasing U_g but is independent of H_s. The values of d_{32} were somewhat higher than the values reported by other investigators. The value of a_i increases with increasing U_g and with decreasing H_s. Present values of compared well with the data reported in literature.

Keywords* : Bubble column, Bubble size, Bubble size distribution, gas holdup, interfacial area, Image processing, Multi-phase system.

I. INTRODUCTION

Bubble columns are extensively used as multiphase reactors in various industries. Mixing and transport properties in bubble columns are due to bubble induced turbulence. Therefore, the design of these reactors requires a good understanding of bubble behavior. One of the important parameters for volumetric mass-transfer coefficient is specific interfacial area, a_i, which depends on the bubble size distribution (BSD). This has led to the need for a greater understanding of the BSD.

Recent investigations in bubble column make use of efficient image analysis techniques for estimating these parameters [1-8]. Zaruba et. al. [8] studied hydrodynamics in a small rectangular bubble column by capturing images at 500 fps for U_g ranging from 0.0005 to 0.004 m s^{-1}. A bubble recognition algorithm was developed and used to tracking every single bubble based on the bright spot at the centre of the bubble. An image processing algorithm generally involves both bubble segmentation and reconstruction techniques. Cordero et. al. [9] used image processing technique to study terminal rise velocity of single bubbles and swarm of bubbles in elastic fluids.

Algorithms such as watershed algorithm [3-4] and the algorithm combining geometrical, optical and topological information [5] were applied to process the dense bubbly flow images in gas-liquid contactors. A robust image measurement technique was proposed to estimate the BSD in high-speed bubbly flows with wide size range of 120 mm–4 mm and void fractions in the range of 0.02–0.7 [1]. It classifies bubbles into different categories based on their morphology and size. Considering that there is an intensity gradient at the center of individual bubble, the bubble clusters are segmented into individual bubbles. The proposed technique was able to capture the bubble characteristics information of all.

The shape of the bubbles and the path were studied with high speed camera using image processing software. A robust and accurate recursive algorithm was developed for concave point extraction. It involved a reconstruction method based on a template database. However, it was illustrated for gas holdup < 0.056 [10]. Measurement of shape of bubbles is also important as bubbles in a bubble column are not perfect sphere. They are deformed while moving in the column. The common shapes of bubbles are nearly spherical, ellipsoidal and spherical cap bubbles. Large bubbles generally are of irregular shape. These bubbles are often described in terms of aspect ratio, which is a measure of deviation from perfect sphere.

BSD is wider at low U_g in comparison with that at high U_g [11]. With the increase of U_g, the BSD shifted from small-to larger diameter bubble. The bubble size increases with the increasing height. The effect of superficial liquid velocity on BSD was not considerably affected. Increasing P and T resulted in BSD shifting from larger-to-smaller diameter bubble. Moreover, BSD was not significant by the properties of the dispersed phase, but mainly affected by the properties of the continuous phase [12]. At low U_g, the bubble characteristics largely influenced by the experimental system taken and not on the operating parameters [8]. In presence of internals, BSD is wider than that for a column without internals [13]. Understanding of BSD helps in understanding flow regime transition [14].

Effect of U_g on BSD, aspect ratio and bubble orientation was studied in an annular gap bubble column for gas holdup varies from 0.029 to 0.096 [7].

Revised Manuscript Received on November 07, 2019.

***** Correspondence Author

Agarwal, N.*, Department of Chemical Engineering and Technology, Indian Institute of Technology (Banaras Hindu University) Varanasi, India. E-mail: neha.agarwal.che10@itbhu.ac.in.

Verma, A. K., Department of Chemical Engineering and Technology, Indian Institute of Technology (Banaras Hindu University) Varanasi, India. E-mail: akverma.che@itbhu.ac.in.

In this range homogeneous flow regime dominates. The image analysis was also used for the evaluation of the U_g at which the transition occurs.

The main problem associated with use if image processing technique to study bubble behavior is overlapping of bubbles. The aim of the present work is develop an image processing technique to identify overlapping bubbles, separating bubble images so that BSD, Sauter mean bubble diameter, gas holdup and a_i may be studied. The effect of U_g and H_s on these parameters was studied so that understanding of bubble behavior is enhanced.

II. EXPERIMENTAL SETUP

A. Experimental Setup

The schematic diagram of the experimental setup is shown in Fig. 1. It consisted of a 2D bubble column having cross section 0.37×0.2×0.02 m made of Perspex. For flow visualization and illumination two walls made of glass. The perforated plate distributor with 200 holes of diameter 0.0015m was used. Air was supplied through a compressor. Air inlet was located at conical shape bottom packed with 0.005 m glass beads, upto a height of 0.05 m. It acted as calming section and used to provide uniform bubbling. A 200 SS mesh was placed over the beads. The gas flow rate was measured using a rotameter.

All the recordings were made by a camera (Nikon, J4 model) placed at a distance of 1.5 m from the column wall. A LED light source (14W) was provided behind the rear wall of the column. Translucent plastic sheet was placed between the light source and the column so that the back of the column was illuminated with diffused light. All experiments were conducted at room temperature. Value of U_g was varies from 0.042 m s^{-1} to 0.168 m s^{-1} and value of H_s varied in the range of 0.20 m to 0.28 m.

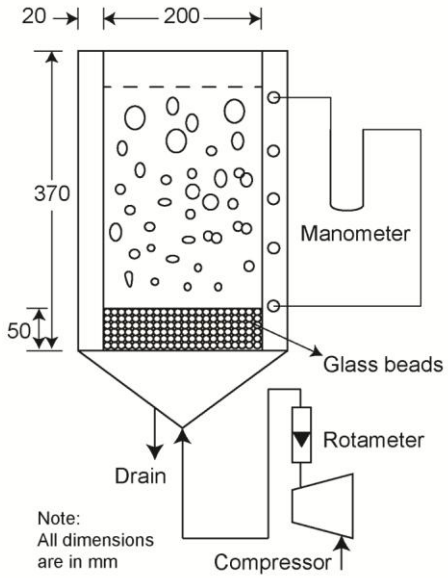

Fig. 1. Experimental set-up

B. Experimental Procedure

Air was introduced in water. Videos were recorded at the rate of 400 fps. Such recordings were made at several U_g and H_s. An algorithm using IP technique was written in MATLAB to analyse these videos. The analysis was performed to determine BSD and its variation with U_g and H_s. The binary image obtained after applying algorithm was used to extract features regarding bubble characteristics. The image processing algorithm consisted of following steps.

1. A frame from movie was extracted.
2. Extracted frame was cropped to contain entire gas-liquid dispersion.
3. Cropped frame was converted to gray-scale image.
4. Contrast of the obtained gray-scale image was enhanced.
5. Obtained image was divided into twenty eight parts, i.e., seven rows and four columns.
6. On each section modified watershed technique was applied.
7. Divided images were reconstructed to get complete binary image of the size equivalent to original image.
8. The bubbles diameter and shape of bubbles were determined using 'regionprops' function of MATLAB.

III. RESULTS AND DISCUSIION

Bubble size was measured from a single frame of the movie. BSD was estimated with the help of IP technique, based on number of bubbles counted in a frame.

A. Bubble Size Distribution (BSD)

BSD for distilled water at U_g = 0.0416 m s^{-1} and H_s = 0.23 m is presented in Fig. 2. It was difficult to measure bubbles of diameter less than 0.002 m. Number of bubbles, N_b, decreases smoothly with increasing d_b. It is a single model function. It can be observed that most of the bubbles are of the diameter about 0.002 m to 0.006 m, though few large bubbles may also be observed. Thus, it is not the case of uniform bubbling. It may be termed as non-uniform (imperfect) homogeneous flow regime or transition to churn-turbulent regime.

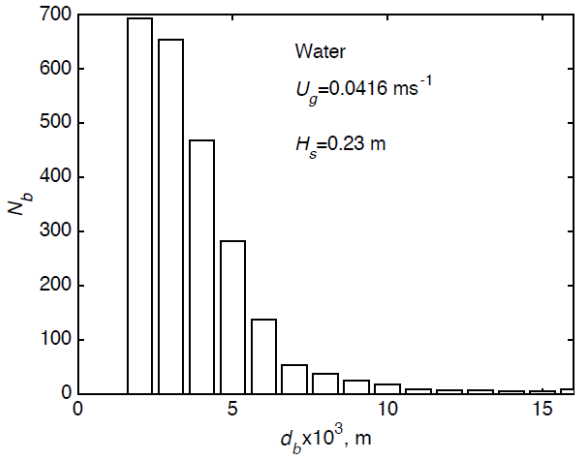

Fig. 2: BSD for distilled water at U_g = 0.0416 m s^{-1}, H_s = 0.23 m.

Effect of U_g on BSD: BSD at H_s = 0.23 m, and for U_g in the range of 0.008 m s^{-1} to 0.058 m s^{-1} is presented in Fig. 3. It clearly shows that the bubbles formed are not of equal size. The striking feature is that the BSD is unaffected by the U_g. There are large number of small bubbles having d_b =0.002 m. Number of bubbles smoothly decreases with increasing bubble diameter. Largest value of N_b at d_b =0.002 m decreases with increasing value of U_g.

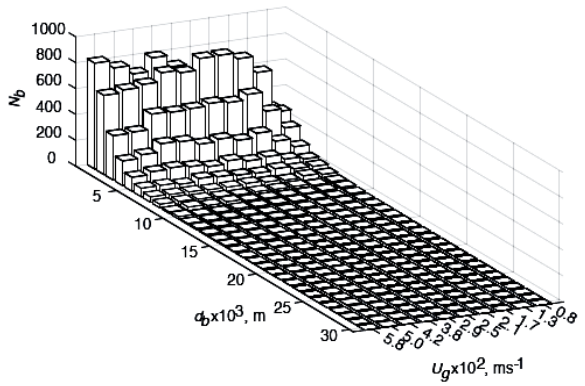

Fig. 3: Effect of U_g on BSD for air-water at H_s = 0.23 m

Effect of H_s on BSD: BSD at U_g = 0.0167 m s^{-1} for H_s in the range of 0.20 m to 0.28 m is presented in Fig. 4. The BSD is similar at all values of H_s. The number of small bubbles seems to increase slightly with increasing value of H_s. BSD at U_g = 0.0417 ms^{-1} for H_s in the range of 0.20 m to 0.26 m is presented in Fig. 5. The trend is similar to that observed in Fig. 3. Thus, it seems that the effect of H_s on BSD is very less. It may be said that very few large bubbles were present for air-water system.

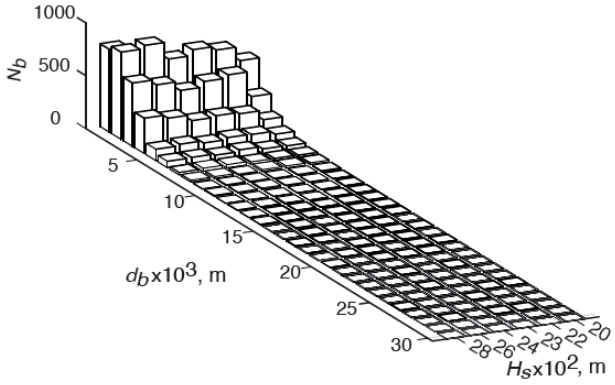

Fig. 4: Effect of Hs on BSD for air-water at Ug = 0.0167 ms-1

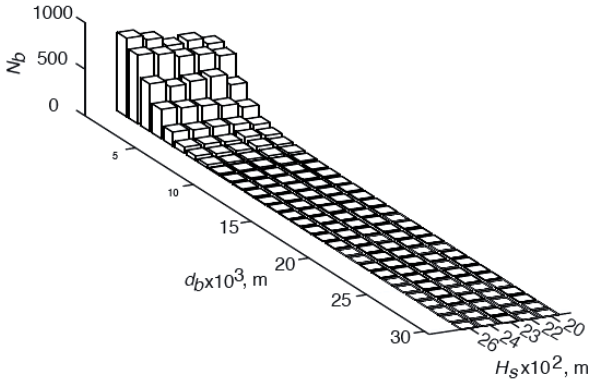

Fig. 5: Effect of Hs on BSD for air-water at Ug = 0.0417 ms-1

From the trends it was observed that the BSD in all cases were single modal. Few large bubbles were also observed. Number of small bubbles increased with increasing value of H_s.

B. *Gas Holdup*

Gas holdup, ε, was estimated using the following expression..

$$\varepsilon = \frac{V_G}{V_G + V_L} \quad (1)$$

Here V_G and V_L are volume of gas and liquid phases in the column respectively. The volume of the gas (air) was estimated by summing volume of all bubbles in the column.

$$V_G = \sum_{N_b} \frac{1}{6} f_{b,i} \left(\pi d_{b,i}^3 \right) \quad (2)$$

where $f_{b,i}$ is the number of i th class of bubbles, $d_{b,i}$ having bubble diameter d_b. The volume of liquid is estimated in terms of H_s and cross sectional area of the column, A_c.

$$V_L = H_s A_c \quad (3)$$

The values of ε as a function of superficial gas velocity for static bed height in the range of 0.20 to 0.28 m for air-water system are shown in Fig. 6. The gas holdup was estimated by taking the value of H_e averaged over all frame for 3 s. The value of gas holdup increases with increasing value of U_g. No effect of H_s on gas holdup is observed upto U_g =0.04 ms^{-1}. Above this value of U_g large difference of ε at various values of H_s can be seen, however no definite trend could be observed. It may be attributed to flow regime transition from homogeneous glow regime to churn-turbulent design.

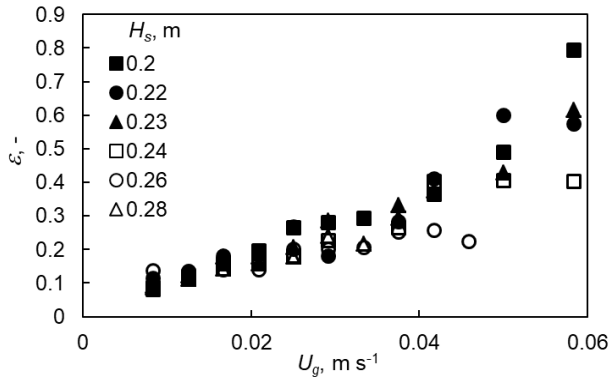

Fig. 6: Variation of ε with U_g at H_s = 0.20 to 0.28 m for air water system

C. *Sauter-mean bubble diameter, d_{32}*

From bubble size data, the value of d_{32} was calculated by

$$d_{32} = \sum_i d_i^3 \Big/ \sum_i d_i^2 \quad (4)$$

where d_i is projected area equivalent diameter of individual bubbles. Values of were evaluated at H_s varies from 0.20 m to 0.28 m and for 0.008 m s$^{-1} \le U_g \le$ 0.058 m s^{-1} for air-distilled water.

Effect of H_s on d_{32}: Variation of d_{32} as a function of U_g and H_s is shown in Fig. 7. The values of d_{32} seem to be independent of H_s. Value of d_{32} increases with increasing U_g. The increase is less for U_g <0.04 ms^{-1}. Above this value of U_g, there is considerable increase of the value of d_{32} indicating that above U_g =0.04 ms^{-1} bubble coalescence starts taking place. The value of U_g =0.04 ms^{-1} is the flow transition velocity.

Data of Cents et al. [15] for air-water system are also shown for comparison. Their data also exhibits increasing d_{32} with increasing U_g. However, present data are about 100%

higher than their data. It could be due to use of sintered porous plate as sparger by Cents et al. [15]. The size of bubbles formed at the sparger in their studies could have been lower than that formed in the present studies.

Pohorecki et al. [16] carried out numerical experiment and proposed the following equation for d_{32} after validating the equation for 7 organic solvents.

$$d_{32} = 0.289\rho^{-0.552}\mu^{-0.048}\sigma^{0.442}U_g^{-0.124} \quad (5)$$

Present values are compared with that predicted using Equation 5 in Fig. 7. The predicted values of d_{32} are lower than present experimental values of d_{32}. Equation 5 predicts d_{32} to decrease with increasing U_g. Similar trends were also reported by Millies and Mewas [17] and Akita and Yoshida [18]. This trend is opposite to the present trend.

Experimental data of Al-Masry et al. [19] for tap water are also shown in the figure. These values also are lower than the present values. It may be due to the fact that the hole diameter used in the sparger in their study was 0.001 m which is lower than that used in the present study.

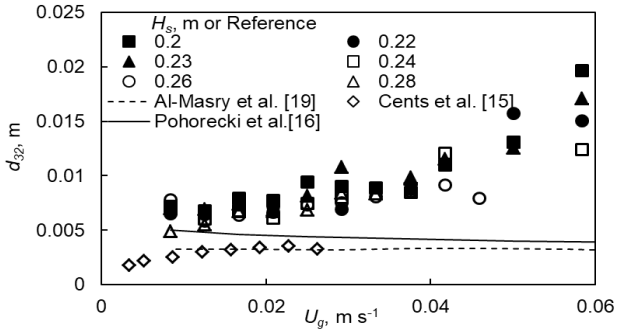

Fig. 7: Variation of d_{32} as a function of U_g and H_s.

D. *Aspect Ratio*

Aspect ratio, E, is estimated as a ratio of minor axis to major axis. Its value is 1 for spherical particles and is less than 1 for other ellipsoids. The value of E for air-water system for U_g = 0.0083 m s^{-1} and H_s = 0.20 m is presented in Figure 8. It is surprising to observe a wide variation in the values of E for even small bubbles. Besagni et al. [7] also used image processing technique to determine the aspect ratio and observed somewhat similar results. It was thought to be due to distortion of the bubbles. It may also be due to overlapping of small bubbles. In case of large deviation in aspect ratio, the mean aspect ratio does not have any meaning and were not determined.

E. *Specific Interfacial Area, a_i*

Specific interfacial area, a_i, in gas-liquid columns can easily be estimated from the value of d_{32} and ε using the following relationship.

$$a_i = 6\varepsilon/d_{32} \quad (6)$$

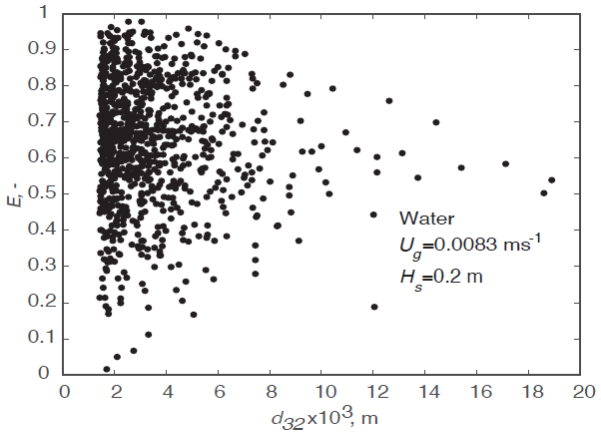

Fig. 8. E for air/water at Ug=0.0083 m s-1, Hs=0.2 m.

Effect of H_s on a_i: Variation of a_i with U_g for static bed height, H_s = 0.20, 0.22, 0.23, 0.24, 0.26 and 0.28 m is shown in Fig. 9. Value of a_i increases with increasing value of U_g and decreasing value of H_s. Experimental values of a_i reported by Cents et al. [15] are also presented in the figure. Present values of a_i are in close agreement to the data of Cents et al [15] upto U_g =0.02 ms^{-1}. Above this value of U_g, present values of a_i are lower than their values. Pohorecki et al. [16] compared several correlations to predict the values of a_i and observed that a_i increases with increasing value of U_g. Following correlation for a_i was proposed [16].

$$a_i = 1120U_g^{0.63} \quad (7)$$

Present data of a_i are about 50 % higher than that predicted from Equation (7). The trend of the data are very much similar to that observed by Pohorecki et al. [16] and Cents et al. [15].

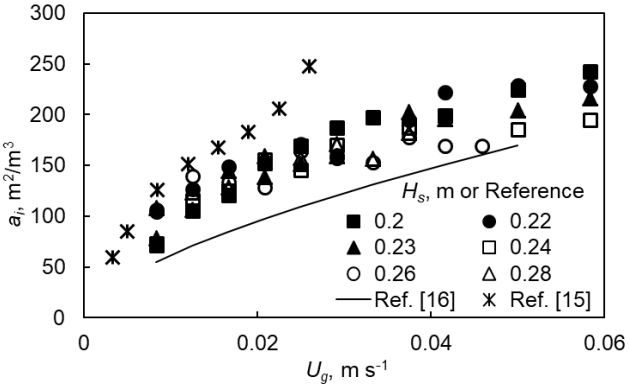

Figu. 9: Variation of a_i with U_g and H_s

IV. CONCLUSION

BSD were measured as a function of superficial gas velocity and static bed height in a bubble column for air-water system using high speed photographic method. The bubble size distribution exhibited mono-modal distribution indicating non-uniform homogeneous bubbling regime. The frames of video were analysed using image processing steps to obtain major and minor axis of elliptical bubbles. Values of d_{32}, ε, and a_i were estimated from the data.

The value of d_{32} increased with increasing U_g but is independent of H_s. The values of d_{32} were somewhat higher than the values reported by other

investigators [15,16,19]. The value of a_i increases with increasing U_g and with decreasing H_s. Present values of compared well with the data reported in literature [15,16].

ACKNOWLEDGMENT

The authors would like to thank the Department of Chemical Engineering and Technology, Indian Institute of Technology (Banaras Hindu University) Varanasi for the all the supports needed to complete this work.

REFERENCES

1. A. Karn, C. Ellis, R. Arndt, J. Hong, "An integrative image measurement technique for dense bubbly flows with a wide size distribution", *Chem. Eng. Sci.* vol. 122, 2015, pp.240–249.
2. F.S. Ahmed, B. A. Sensenich, S.A. Gheni, D. Znerdstrovic, M. H. Al-Dahhan "Bubble Dynamics in 2D Bubble Column: Comparison between high-speed camera imaging analysis and 4-point optical probe", *Chem. Eng. Commun*. vol. 202, 2015, pp. 85–95.
3. Y.M. Lau, N.G. Deen, J.A.M. Kuipers, "Development of an image measurement technique for size distribution in dense bubbly flows" *Chem. Eng. Sci.* vol. 94, 2013a, pp.20–29.
4. Y.M. Lau, K. T. Sujatha, M. Gaeini, N.G. Deen, J.A.M. Kuipers "Experimental study of the bubble size distribution in a pseudo-2D bubble column", *Chem. Eng. Sci*. vol.98, 2013b, pp. 203–211.
5. Y. Fu, Y. Liu, "Development of a robust image processing technique for bubbly flow measurement in a narrow rectangular channel", *Int. J. Multiphase Flow*. vol. 84, 2016, pp.217–228.
6. A. Zaruba, E. Krepper, H. M. Prasser, E. Schleicher, E. "Measurement of bubble velocity profiles and turbulent diffusion coefficients of the gaseous phase in rectangular bubble column using image processing", *Exp. Therm. Fluid Sci*. vol. 29, 2005, pp.851–860.
7. G. Besagni, F. Inzoli, "Bubble size distributions and shapes in annular gap bubble column", *Exp. Therm Fluid Sci.* vol. 74, 2016a, pp.27–48.
8. G. Besagni, F. Inzoli, "Comprehensive experimental investigation of counter-current bubble column hydrodynamics: Holdup, flow regime transition, bubble size distributions and local flow properties", *Chem. Eng. Sci.* vol. 146, 2016b, pp.259–290.
9. J.R.V. Cordero, D. Sámano, R. Zenit, "Study of the properties of bubbly flows in Boger-type fluids", *J. Non-Newtonian Fluid Mech*. vol. 175–176, 2012, pp.1–9.
10. S. Zhong, X. Zou, Z. Zhang, H. Tian, "A flexible image analysis method for measuring bubble parameters", *Chem. Eng. Sci*. vol. 141, 2016, pp.143–153.
11. X. Guan, N. Yang, "Bubble properties measurement in bubble columns: From homogeneous to heterogeneous regime", *Chem. Eng. Res. Des*. vol. 127, 2017, pp. 103–112.
12. D. Feng, J-H. Ferrasse, A. Soric, O. Boutin, "Bubble characterization and gas–liquid interfacial area in two phase gas–liquid system in bubble column at low Reynolds number and high temperature and pressure", vol. 144, 2019, pp. 95-106.
13. Y.M. Lau, F. Moller, U. Hampel, M. Schubert, "Ultrafast X-ray tomographic imaging of multiphase flow in bubble columns – Part 2: Characterisation of bubbles in the dense regime", *Int. J. Multiphase Flow*, vol. 104, 2018, pp. 272-285.
14. A. H. G. Cents, D. J. W. Jansen, D.W.F. Brilman, G. F. Versteeg," Influence of Small Amounts of Additives on Gas Hold-Up, Bubble Size, and Interfacial Area", *Ind. Eng. Chem. Res.* vol. 44, 2005, pp.4863-4870.
15. R. Pohorecki, W. Moniuk, A. Zdrójkowski, "Hydrodynamics of a bubble column under elevated pressure", *Chem. Eng. Sci.* vol. 54, 1999, pp. 5187-5193.
16. M. Millies, D. Mewas, "Interfacial area density in bubbly flow", *Chem. Eng. Process.* vol. 38, 1999, pp. 307–319.
17. K. Akita, F. Yoshida, "Bubble size, interfacial area, and liquid-phase mass transfer coefficient in bubble columns", *Ind. Eng. Chem. Process Des. Dev*. vol. 13(1), 1974, pp. 84-91.
18. W. A. Al-Masry, E. M. Ali, "Identification of hydrodynamics characteristics in bubble columns through analysis of acoustic sound measurements—Influence of the liquid phase properties", *Chem. Eng. Process.* vol. 46, 2007, pp.127–138.

AUTHORS PROFILE

Neha Agarwal is research scholar in the Department of Chemical Engineering and Technology at Indian Institute of Technology (Banaras Hindu University) Varanasi. She has obtained his M.E degree from IIT (BHU) Varanasi. She is currently working on measurement of bubble behavior in bubble columns using image processing tools for photographic method.

Ashok Kumar Verma is professor in the Department of Chemical Engineering and Technology at the Indian Institute of Technology (Banaras Hindu University) Varanasi. He holds a BSc from Allahabad University, a BE in chemical engineering from University of Roorkee (now Indian Institute of Technology, Roorkee), an ME in chemical engineering from the Indian Institute of Sciences, Bangalore, and a PhD in chemical engineering from the Indian Institute of Technology, Kanpur. He joined the Institute of Technology, Banaras Hindu University, Varanasi in 1984. He worked at University of Chicago, Illinois, USA for post-doctoral research during 1987-88. He is author of book "Process Modelling and Simulation in Chemical Biochemical and Environmental Engineering" published by CRC press, Boca Raton, USA. He has also authored or co-authored numerous papers/book chapters in journals, and national and international proceedings. He has presented papers in national and international conferences. His current research area includes application of acoustic signal analysis, image processing and artificial intelligence in various fields of chemical engineering, modelling and simulation of multiphase systems.